

ОБЪЕДИНЕННЫЙ
ИНСТИТУТ
ЯДЕРНЫХ
ИССЛЕДОВАНИЙ

Дубна

97-8

E15-97-8

A.E.Drebushko, V.V.Filchenkov, A.I.Rudenko

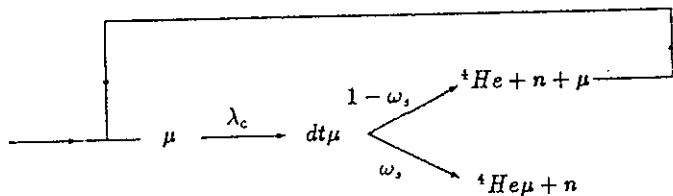
ANALYSIS METHODS IN THE NOVEL MANNER
OF THE STUDY
OF MULTIPLE MUON CATALYSIS PROCESS

Submitted to «Nuclear Instruments and Methods A»

1997

I. Introduction

Study of the muon catalyzed fusion (MCF) reactions is now of great interest and is carried out in many laboratories of the world. A wide experimental program of such investigations is now realized in the frame of the large international project TRITON aimed to measure the characteristics of the d+t fusion cycle



in the double D/T and the triple H/D/T mixture of high density (up to the liquid hydrogen density, LHD). The main parameters to be measured are the absolute neutron yield per muon (Y_n), the fusion cycle (λ_c) and the probability of muon sticking to helium (ω_s). According to this we shall follow the way of an "effective" analysis where the simplest model reflected in the scheme is considered.

The experimental method is based on the original ideas of the authors of Refs. [1], [2], [3]. In the paper [1] the time spectrum of the last detected neutron relative to muon decay was suggested to be measured. This spectrum is a sum of two exponents [2], [3]:

$$dN/dt = (\lambda_0/\lambda_n) \cdot [w \cdot \lambda_c \cdot \exp(-\lambda_0 \cdot t) + \epsilon_n \cdot \lambda_c \cdot (1 - w) \cdot \exp(-(\lambda_0 + \lambda_n) \cdot t)]. \quad (1)$$

Here $\lambda_0 = 0.455 \mu s^{-1}$ is the muon decay rate, and λ_n is defined as $\lambda_n = (\epsilon_n + w - \epsilon_n \cdot w) \cdot \lambda_c$, ϵ_n is the neutron detection efficiency, w is the effective sticking probability taking into account the muon sticking in the d+d and t+t accompanied reactions. The ratio of the amplitudes of the slow and fast exponents determines the value of w : $A_s/A_f = w/\epsilon_n(1 - w)$.

Another idea [2] is to register the neutron multiplicity (number of detected neutrons, k , per muon) distribution in some time interval T during which muon does not disappear. This distribution is a sum of two terms. One of them, the Gaussian (Poisson), $g(k; m)$, with the mean $m = \epsilon \cdot \lambda_c \cdot T$, corresponds to events without sticking and another one, $f(k)$, is caused by the "sticked" events:

$$N(k) = N_1 \cdot [f(k) + (1 - \omega/\epsilon_n)^m \cdot g(k; m)]. \quad (2)$$

Here N_1 is the total number of the first detected neutrons in the time interval T (the sum of $N(k)$). Under the condition $m \gg 1$ the function $f(k)$ is described by the formula $f(k) = y_{k-1} - y_k = y_1 \cdot [1 - y_1 \cdot (1 - \omega)] \cdot [y_1 \cdot (1 - \omega)]^{k-1}$, where y_1 is the relative yield of the first detected neutrons. It is important that the function $f(k)$ does not depend on λ_c for events selected according to the above-mentioned criterion $t_c > T$. As is shown in [2] the analysis of the distributions $N(k)$ makes it possible to determine the parameters ω/ϵ and λ_c .

Finally, the time distribution of all detected neutrons currently analyzed in the MCF experiments will be measured. They have the well known form

$$dN/dt = \epsilon \lambda_c \cdot \exp[-(\lambda_0 + \omega \lambda_c)]. \quad (3)$$

As follows from theory and experiment, the sticking probability is to be $\omega \approx 0.005$. Under the optimal D/T conditions (high density and high tritium concentration) the value of the cycling rate can achieve $100 - 150 \mu s^{-1}$. Large "full absorption" neutron detector (ND) [4] is used to register 14 MeV neutrons from the d+t fusion reaction. It consists of two identical parts (11 l of each) symmetrically located around the target. Its detection efficiency is 2x(10-15) percent.

The "physical" distributions (1), (2), (3) have been considered in [1], [2], [3]. However, in the real experimental conditions, where the value of the measured neutron yield can be $Y_n^{exp} \approx 20 - 30 / \mu s$, they can be substantially distorted due to the *pile up* effects. To discriminate these distortions one decides to measure the ND charge spectra [3] instead of the currently measured distributions of the number of events. Flashes ADC 256 (amplitude) x 2048 (time) with a strob pulse frequency 100 Mc are used for this purpose. But some distortions can remain since the time interval between strob pulses is approximately the same as the ND signal duration [5]. Moreover, distortions would be also caused by a threshold in the amplitude measurements introduced to discriminate background. The most serious problem is to provide the correct charge calibration being important for the absolute yield measurement.

To consider these problems we have developed a package of the Monte-Carlo programs simulating the measurements with FADC. Special attention was paid to the charge calibration procedure. Using the programs we tried to estimate the possible distortion in the measured spectra in dependence on the detector signal parameters, neutron multiplicity and threshold. The simulated spectra were fitted with formula (1-3) for this purpose. Finally, these programs are shown to be very useful for preparing the methods of on-line control and analysis. This turns to be very important due to the extreme difficulty in providing the appropriate conditions (high intensity pulsed source) for testing measurements before the experiment with tritium.

II. Calculation programs

The structure of the calculation package is shown in Fig. 1. The first box is related to the simplified kinetics of the MCF process. The current parameters are the deuterium and tritium concentrations, the neutron detection efficiency, ω and other characteristics of the process. Each individual muon is under control. The competition between the d+t fusion reaction and mu-decay is simulated successively from cycle to cycle. The muon sticking to helium, which stops the catalysis, is checked. The time of each neutron from the MCF reaction series is determined in this part.

In the next box ("Detector") one finds out whether neutron is detected or not. If yes, then one determines the value of energy released in the scintillator. The uniform recoil proton energy spectrum was used for this in the simplest case. The neutron detector signal was formed according to the study of its shape in Ref. [5]. The possibility of its transformation was provided. The example of the detector signal series (the first 400 ns) caused by one muon is given in Fig. 2.

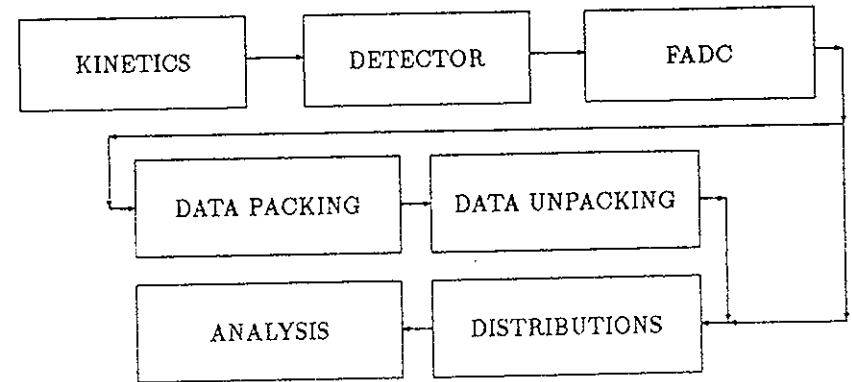


Figure 1: Structure of the calculation complex.

The third block imitates the FADC. Here the detector signals are scanned with strob pulse series with a random phase. We will call the amplitude codes obtained we will call the amplitudes and its sum the charge. Different values of the amplitude threshold were used in the calculations. Series of successive codes which of them is above threshold will be called the *cluster* and their sum the *cluster charge*.

The next two blocks of the programs are designed to "pack" (and "unpack") data. These programs were necessary to create the on-line control methods and check them before the experiment. Finally, in the last blocks different distributions were accumulated and analyzed.

The main programs were tested in the "event mode", where the calculated distributions should obey to the formula (1)-(3). For this purpose the ND detector signal was accepted as the delta function (in time) with the charge equal to unity. In the "charge mode" (with FADC) the detector signal was described as

$$s_0(t) = t \cdot \exp[-t/\tau]; \quad \tau = 10 \text{ ns} \quad (4)$$

broken off at $\Delta t = 30 \text{ ns}$ or 50 ns . Some special types of the shape (for instance, a triangle) were also considered.

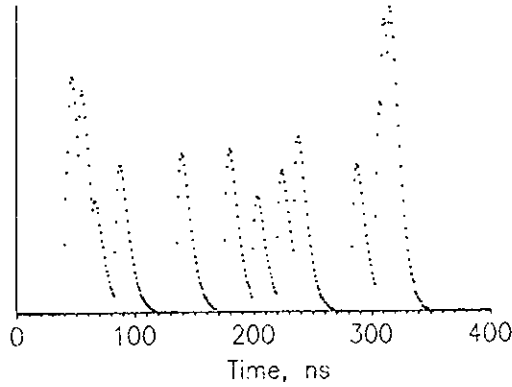


Figure 2: Example of the ND signal series.

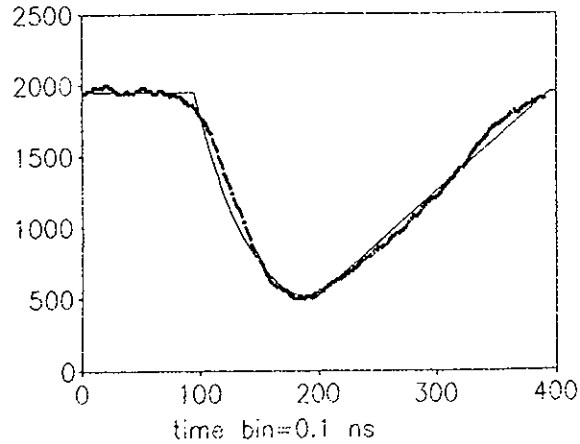


Figure 3: Shape of the ND signal used in the calculations. The dashed curve corresponds to the "original" signal of shape (4) broken off at 50 ns . The circles represent the measurements and solid curve is the approximation function (5) for the shortened signal.

After all calculations one decides to shorten the "original" ND signal (4) to provide more correct time measurements. One finds out that the most simple way is to make

this as follows

$$s(t) = s_0(t) \text{ for } t = 0 \div \tau; \quad s(t) = s_0(\tau) \cdot [1 - (t - \tau)/\Delta t] \text{ for } t = \tau \div \tau + \Delta t \quad (5)$$

with $\tau = 10 \text{ ns}$ and $\Delta t = 20 \text{ ns}$. Therefore we repeated the main calculations for this signal shape. Fig. 3 shows the shape of the ND signal. The dashed curve corresponds to Eq. 4 and the solid one to Eq. (5). Circles are the measurements at the transformed signal. As is seen, the approximation function (5) is described well the real signal.

In most cases the values

$$\epsilon = 0.3, \quad \lambda_c = 100 \mu\text{s}^{-1}, \quad \omega = 0.005 \quad (6)$$

were used. Of course, they correspond to an extreme case (really, as expected, $\epsilon\lambda_c \leq 15 \mu\text{s}^{-1}$), but it allows an estimate of the most possible systematic distortions due to the pile up effects.

III. Results

Let us first consider the "usual" time distributions of all detected neutrons.

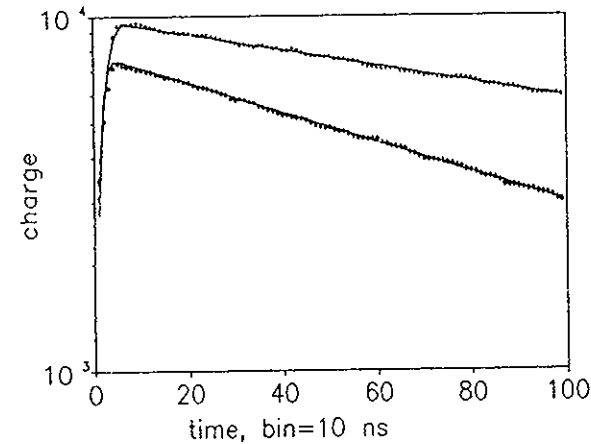


Figure 4: Time distributions of all detected neutrons. The upper spectrum was simulated for $\epsilon\lambda_c = 3 \mu\text{s}^{-1}$ (low multiplicity) and the lower one for $\epsilon\lambda_c = 30 \mu\text{s}^{-1}$ (high multiplicity). Curves are the appropriate fitting functions.

Use of the "single mode" when only the first code (above the threshold) in the cluster is considered, results in substantial violation of the time spectrum shape. Obviously, in the limit of very high neutron multiplicity events will be accumulated only in the first channel (channels) of this spectrum. Thus we must use all codes. This superfluous information leads to some spectrum distortions, of the type of differential nonlinearity, which manifests itself mostly for low statistics. Besides, the problem of correct determination of uncertainty in the spectrum parameters found from the standard fit procedure requires special consideration.

In the present work our main aim is to estimate possible systematic errors in the spectrum slope values. In Fig. 4 the time distributions of all detected neutrons are presented for high ($30 n/\mu$) and low ($6 n/\mu$) neutron multiplicity. The lower spectrum corresponds to the values (6) and statistics $N_\mu = 10^4$, the upper spectrum was calculated with $\epsilon\lambda_c = 3 \mu s^{-1}$ and $N_\mu = 8 \cdot 10^4$. Both distributions were normalized to the average "unit charge" $q = Q/N_n$, where Q is the total charge and N_n is the total number of detected neutrons, and fitted with expression (3) with finite time resolution taken into account [6]. Fitting functions are shown in the figure by curves. As can be seen from the figure, some distortions are manifested in this rather low statistics. The optimal values of the exponent slope were found to be

$$0.964(3) \mu s^{-1} \text{ (expected value } 0.955 \mu s^{-1}) \text{ and } 0.508(3) \mu s^{-1} \text{ (} 0.505 \mu s^{-1})$$

for the high and low cycling rate respectively. Thus the systematic shift in the exponent slope does not exceed one percent. To exclude the possible influence of the factor of the finite duration of the ND signal compared with the strob pulse interval we check our fit with the distributions summarized over four channels. While this procedure was made the value of χ^2 becomes close to the expected one, that provides the correct determination of the parameter uncertainties found in the fit.

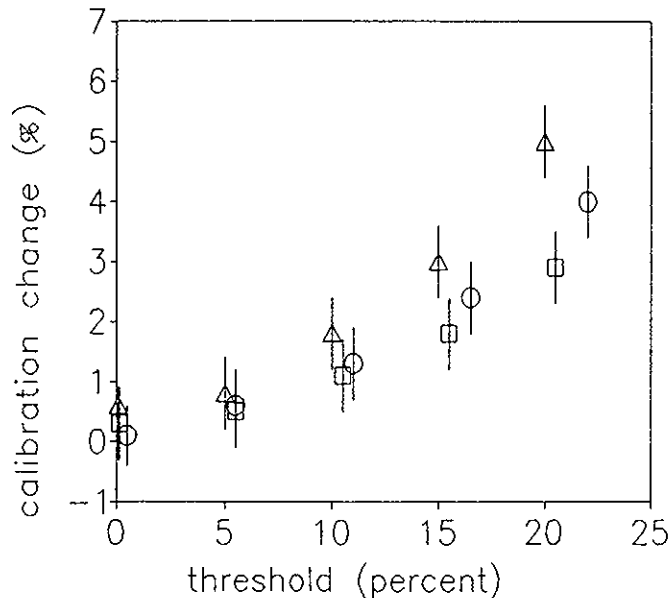


Figure 5: Values of $\delta q = [Q/N_n(\epsilon\lambda_c = 20 \mu s^{-1})] / [Q/N_n(\epsilon\lambda_c = 2 \mu s^{-1})] - 1$ as a function of the amplitude threshold. Squares and triangles correspond to a "usual" amplitude threshold for the original (4) and shortened (5) ND signal respectively. Circles reflect the calculations with shortened signal and the amplitude restriction inside the cluster.

Experimentally, the charge calibration procedure can be done in the exposures with low neutron multiplicity where the pile up effects are poor and the neutron number

can be reliably determined. The question is how this calibration is kept for exposures with high neutron multiplicity, especially if one uses a rather high threshold. To check it we made the calculations for high ($30 n/\mu$) and low ($5 n/\mu$) multiplicity at different threshold values. The results are presented in Fig. 5.

The relative change in the unit charge

$$\delta q = [Q/N_n(\epsilon\lambda_c = 20 \mu s^{-1})] / [Q/N_n(\epsilon\lambda_c = 2 \mu s^{-1})] - 1$$

is plotted in it as a function of the relative (to the maximum signal amplitude in the proton recoil spectrum) threshold. As is seen from the figure, the change in the calibration value is only one-two percent for the relative threshold $\approx 10\%$.

Another method of charge calibration follows from consideration of the neutron multiplicity distribution (2). The parameter m is the mean value of the Gaussian $m = \epsilon\lambda_c T$ and at the same time it determines the relative part of the Gaussian component $(1 - \omega/\epsilon)^m$. This fact is well manifested in Fig. 6, where the multiplicity distributions are presented for three values of T : $1 \mu s$ (a), $2 \mu s$ (b) and $4 \mu s$ (c). One can see that with changing peak position its relative part also changes.

While the charge distribution is analyzed with formulae (2) the mean of the Gaussian should be multiplied by the unit charge: $m \rightarrow M = m \cdot q$ ($q = Q/n$). But the relative part of the Gaussian does not depend on the charge and is determined by the "physical" quantity m . Thus, fit of the measured distribution with independent optimization of the parameters M and m makes it possible to obtain the value of q .

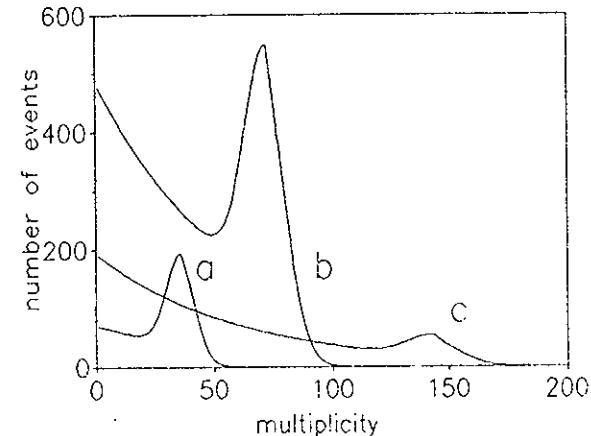


Figure 6: Neutron multiplicity distributions accumulated for the time interval $T = 1 \mu s$ (a), $T = 2 \mu s$ (b) and $T = 4 \mu s$ (c).

Thus, the main characteristics of the d-t fusion cycle λ_c , ω and $Y_n = \epsilon\lambda_c / (\lambda_0 + \omega\lambda_c)$ can be determined, in principle, from the analysis of the multiplicity distribution.

Figure 7 shows the multiplicity distributions simulated for $T = 2 \mu s$ with the values (6) λ_c , ϵ and ω . The dashed curve corresponds to the "events mode". The spectrum obtained in the "charge mode" is shown by circles. It is scaled according to the

calculated value of the unit charge. The solid curve is function (2) with the optimal parameters found from the fit.

The expected values of those parameters are

$$m = 60 \text{ and } \omega/\epsilon = 0.0167.$$

The values found from the analysis of the "physical distribution" turned out to be

$$m = 59.7 \pm 0.2, \quad \omega/\epsilon = 0.0171 \pm 0.02$$

which are very close to the expected ones.

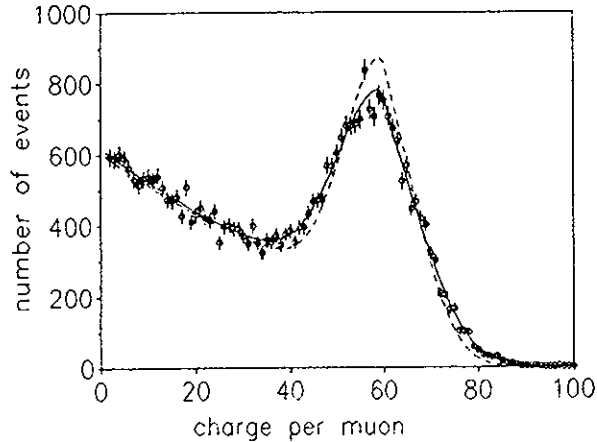


Figure 7: Neutron multiplicity distributions simulated for $T = 2 \mu s$ with λ_c , ϵ and ω values (6) in the "charge mode" (circles) and "event mode" (dashed curve). The solid curve corresponds to formulae (2) with the optimal parameters found from the fit.

If one independently vary the parameters m and $M = mq$ (the expected value for the normalized spectrum is $q = 1!$), one obtains

$$M = 59.6 \pm 0.2, \quad \omega/\epsilon = 0.0179 \pm 0.008, \quad m = 54.1 \pm 4.6.$$

As is seen, the accuracy changes for the worse, especially for the value of m . This is due to correlation between two parameters (m and ω/ϵ) determining the relative part of the unsticked (sticked) events. (As follows from the further study, expansion of the observation interval T allows improvement of the accuracy in $\xi = \omega/\epsilon$ and m . For $m = 109$ it is $\delta_\xi/\xi \simeq 2\%$ and $\delta_m/m \simeq 4\%$).

Independent measurement of the unit charge q can improve the accuracy in the value of ω . Besides, we can also use the value of $\epsilon\lambda_c$ found from the analysis of the " $t_e - t_n$ " distribution and thus to extract the value of q from the mean of the Gaussian: $m = \epsilon\lambda_c T$.

Accurate measurements of the " $t_e - t_n$ " distribution with FADC is the subject of intensive discussions among the members of the MCF community because the expected

value of fast exponent slope $\epsilon\lambda_c$ in the expression (1) is of the order of the ND signal duration and strob pulse interval. To study the problem we calculated this spectrum for various conditions. An example the spectrum obtained for the values (6) and the ND signal duration $30 ns$ is shown in Fig. 8 (circles). To accumulate it we use the time difference between the mu-decay electron and the last FADC code above the threshold.

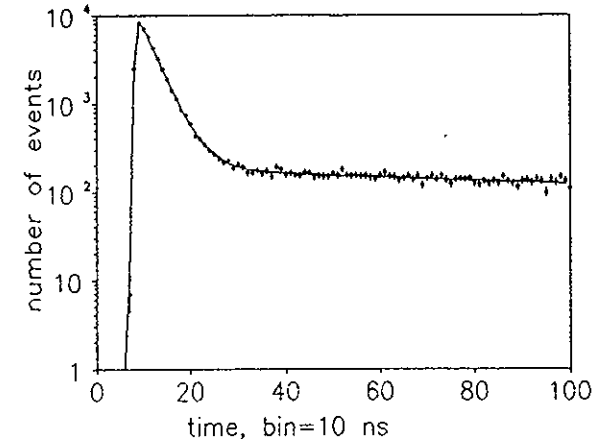


Figure 8: Time spectrum of the last detected neutrons relative to the muon decay electron (points). The curve is function (1) with the optimal parameters found from the fit.

The simulated distributions were fitted with expression (1) with account of the finite time resolution factor. Both this resolution and the time zero (t_0) position were found from the fit. The expected values of the main parameters are the fast exponent slope $\lambda_f = \lambda_0 + \epsilon\lambda_c = 30.5 \mu s^{-1}$ and the ratio between the slow and fast component amplitudes $A_s/A_f = \omega/\epsilon = 0.0167$. The results obtained are placed in the Table I.

To check the kinetic simulation and the fit procedure, the results were firstly obtained for the "event mode". They are presented in the third column of the Table I. The agreement with the expected values is within 1–2%. In the next three columns we show the parameters found from the analysis of distributions simulated for real conditions with FADC. As is seen from the table, the use of FADC results in some systematic shifts in the values of parameters, most clearly manifesting themselves for a long ND signals.

Table 1. Parameters of the " $t_e - t_n$ " - distribution.

Parameter	Expected value	Fit for the "event mode"	Fit for the "charge mode"		
			Signal duration		
			30 ns	50 ns	70 ns
A_s/A_f	0.0167	0.0171(3)	0.0173(2)	0.0176(2)	0.0185(2)
$\lambda_f, \mu s^{-1}$	30.8	30.6(3)	29.5(2)	28.8(2)	27.3(2)

Another important problem is related to employment of the detection efficiency calculations. Currently, to check them and to determine the efficiency loss due to

threshold, we reconciled the calculated response function of the recoil proton energy with the measured one. At that we must be sure in the correct measurements of the ND detector charge being equivalent the proton energy. To provide this, first of all we must perform the measurements in experimental conditions corresponded the low neutron multiplicity. However, while the charge measurements are made with FADC at the strob pulses interval just compared with the ND signal duration some distortions in the charge measurements are inevitable even in this extreme case. Of course, due to statistical effects they are compensated and result mostly in the worsening of the amplitude resolution. But some systematic distortions are conserved especially if a rather high amplitude threshold is taken.

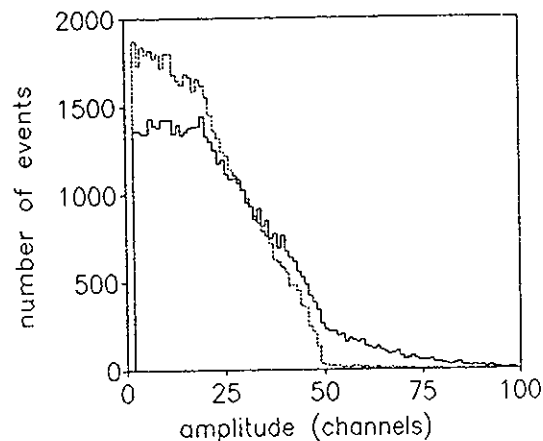


Figure 9: FADC amplitude spectrum calculated for ND signals of shape (4) uniformly distributed in amplitude. The solid histogram corresponds to high neutron multiplicity $30 n/\mu$ and the dashed one to $3 n/\mu$.

To study the problem we have calculated the amplitude and charge distributions for different conditions. The original response function was taken to be uniformly distributed from zero to some maximum value or put as a some fixed value. Figure 9 shows the FADC amplitude distribution simulated for the ND signals of "usual" shape (4) uniformly distributed in amplitude. As expected, reproduction of the original spectrum is unsatisfactory in this case.

The charge measurements (sum of the amplitude codes inside the cluster) should reproduce the original spectrum much more correctly. First of all, to check the programs, we considered the ND signal shape as a triangle with the base equal to the double strob pulse interval (20 ns). In this ideal case the charge value of a separate signal should not depend on the phase of the strob pulse series. The appropriate spectra are shown in Fig. 10 for low ($2 n/\mu$) and high ($20 n/\mu$) neutron multiplicity. As is seen from the figure, for low multiplicity the spectra obtained with FADC reproduce the initial ones rather well.

At the next stage we considered the charge distributions for the real shape of the

ND signal. Since possible distortions are expected to be as large as the ND signal is short, we present the results for the shortened signal of shape (5). The calculations were made for the uniform amplitude distribution with and without the amplitude threshold. Solid histograms in Fig. 11 represent the distribution obtained for the minimal threshold equal to 2% relative to the maximum amplitude value of the ND signal. Its comparison with the appropriate spectrum of Fig. 10,c shows that measurements with FADC with the real signal lead to some deterioration of the charge resolution under satisfactory reproduction of the spectrum shape, though.

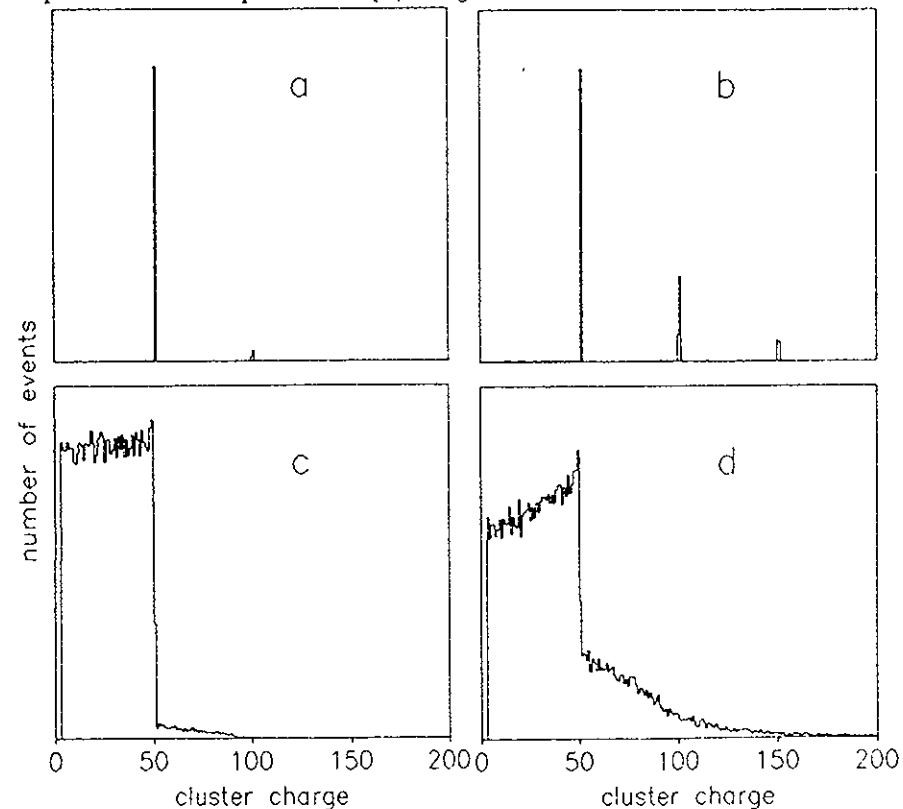


Figure 10: Charge distributions obtained for a triangular signal. The upper spectra correspond to the constant amplitude and the lower ones to the uniformly distributed one. The left pictures (a, c) are related to low neutron multiplicity ($2 n/\mu$) and the right ones (b, d) to high multiplicity ($20 n/\mu$).

From the physical point of view, the charge (energy) threshold should be introduced to eliminate events from the accompanying d-d fusion reaction (the maximum recoil proton energy is equal to 0.7 MeV of an equivalent electron energy, E_{ee}) and low energy background. Call that the appropriate energy for the d-t fusion reaction to be studied is $E_{ee} \approx 7 \text{ MeV}$. As follows from our consideration, the use of the "usual" amplitude limitation leads to substantial distortions of the final charge distributions (see Fig. 11, b).

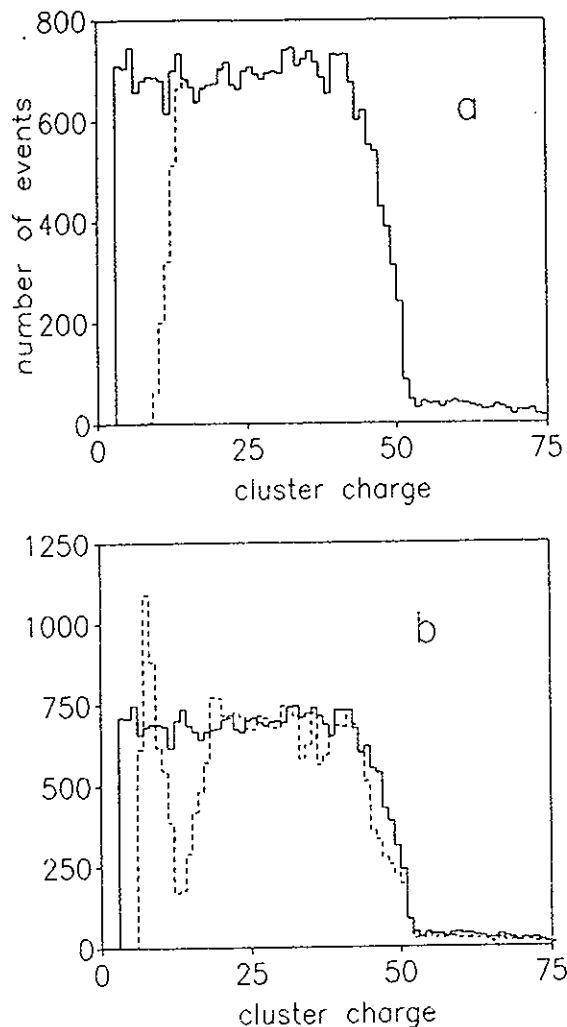


Figure 11: Charge spectra calculated for the ND signals of shape (5) with the uniformly distributed amplitude. Solid histograms are obtained with a low threshold and the dashed ones correspond to a 20% threshold relative to the maximum amplitude value. Case (a) corresponds to amplitude restriction inside the cluster and variant (b) to "usual" amplitude threshold.

Therefore we used the following algorithm. Producing charge spectra we controlled the maximum value of the amplitude inside the cluster and considered only those cluster charges for which this amplitude exceeded the chosen threshold value. As is seen from Fig. 11, a, this provides conservation of the charge spectrum shape except for low channels.

Figure 12 shows the results of the direct experimental check of our charge measurement methods. The spectra shown in it were obtained with the γ -source ^{60}Co . The histogram represents the measurement with FADC and circles are the same for a "usual" charge digitizer (QCD). As can be seen from the figure, there is very good agreement between both spectra with exception of the lowest charge values (in this case it is due to the threshold effect in the measurements with QCD).

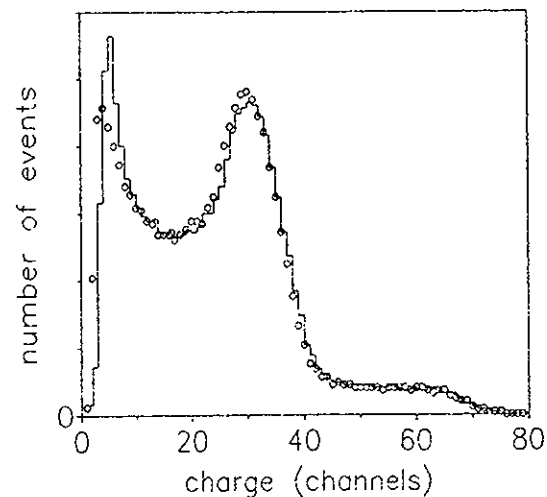


Figure 12: Charge distributions obtained with the γ -source ^{60}Co . The histogram represents the measurement with FADC and circles for that with an "usual" charge digitizer.

III. Conclusion

The μCF experiment has been modelled, starting with the kinetics of the process and ending with the analysis of the data obtained. The results give us an assurance that we are now able to operatively analyze the data to be measured in the planned experiment on the determination of the main MCF parameters in the liquid D/T mixture. The developed method allows estimation of uncertainties in this parameters for real experimental conditions. It follows from our consideration that the neutron multiplicity Y_n , cycling rate λ_c and sticking probability ω can be determined with an accuracy of few percent.

The authors are indebted to A.D. Konin, V.T. Sidorov and V.G. Zinov for helpful discussions. The financial support of the International Science and Technology Center (ISTC) is gratefully acknowledged.

References

- [1] V.G. Zinov, *Muon Cat. Fusion*, **7** (1992) 419.
- [2] V.V. Filchenkov, *Muon Cat. Fusion*, **7** (1992) 409.
- [3] D.L. Demin et al, Contributed paper to the X-th Int. Symposium on Muon Catalyzed Fusion, Dubna, 19-24 June 1995; to be published in *Hyp. Int.*, 1996.
- [4] V.P. Dzhelepov et al, *Nucl. Instr. and Meth.*, **A 256** (1988) 634.
V.V. Filchenkov, A.D. Konin, A.I. Rudenko,
Nucl. Instr. and Meth., **A 294** (1990) 504.
- [5] V.A. Baranov, V.V. Filchenkov, A.D. Konin, V.V. Zhuk,
Preprint JINR **R13-95-261**, Dubna, 1995;
Nucl. Instr. and Meth., **A 374** (1996) 335.
- [6] V.P. Dzhelepov et al., *Zh. Eksp. Teor. Fiz.*, **101** (1992) 1105,
Sov. Phys. JETP, **74** (1992) 589, *Muon Cat. Fusion*, **7** (1992) 387.

Received by Publishing Department
on January 15, 1997.